Afshar Vahid, Shahraam; Ruan, Yinlan; Warren-Smith, Stephen; Monro, Tanya Mary. Enhanced fluorescence sensing using microstructured optical fibers: a comparison of forward and backward collection modes, *Optics Letters*, 2008; 33 (13):1473-1475.

Enhanced fluorescence sensing using microstructured optical fibers: a comparison of forward and backward collection modes

Shahraam Afshar V.,* Yinlan Ruan, Stephen C. Warren-Smith, and Tanya M. Monro

Centre of Expertise in Photonics, School of Chemistry and Physics, University of Adelaide, Adelaide, South Australia 5005, Australia

**Corresponding author: shahraam.afshar@adelaide.edu.au*

Received February 20, 2008; revised May 9, 2008; accepted May 9, 2008; posted May 21, 2008 (Doc. ID 92951); published June 24, 2008

A general model of excitation and fluorescence recapturing by the forward and backward modes of filled microstructured optical fibers (MOFs) is presented. We also present experimental results for both backward and forward fluorescence recapturing within a MOF as a function of fiber length and demonstrate a good qualitative agreement between the numerical model and experimental results. We demonstrate higher efficiency of fluorescence recapturing into backward modes in comparison with that of forward modes. © 2008 Optical Society of America

OCIS codes: 060.2370, 060.4005, 280.1415.

Microstructured optical fibers (MOFs) have recently attracted considerable interest as ideal tools for chemical or biological sensing ([1], and references therein), since a significant portion of the guided light can overlap with chemical–biological materials filled into the holes of the fibers. The sensing mechanism can be either based on absorption or fluorescence spectroscopy. Although a range of MOF variants of fluorescent-based sensors have been reported ([1], and references therein), the benefits that can be obtained using MOFs are far from being realized, largely due to the lack of a formalism for predicting and thus optimizing the measurable fluorescence power. Recently, we reported a general model for calculating the sensitivity of fluorescence-based sensing using filled MOFs [1]. The model is based on the excitation of the sensing material by the guided modes of the MOFs and the recapturing of their fluorescence emission within the forward propagating modes (the forward fluorescence capture fraction Φ_F) considering losses at both excitation and fluorescent frequencies. It demonstrates [1] that the light–matter overlap alone does not determine the optimal fiber choice as is usually assumed and that fiber designs with subwavelength features and high index glass exhibit localized regions of high intensity [2,3], which lead to enhanced fluorescence recapturing and hence higher sensing sensitivity.

In this Letter we have advanced the model presented in [1] to include the capturing of fluorescence emission into the backward propagating modes (the backward fluorescence capture fraction Φ_B). We then demonstrate that Φ_B and Φ_F show different behavior as a function of fiber length, where Φ_B can be more than 15% higher than the Φ_F, and discuss the advantages of Φ_B over those of Φ_F. Also by using an aqueous solution with quantum dots [4,5], which experience negligible photobleaching, we experimentally confirm the behavior of Φ_F and Φ_B as a function of fiber length for the first time, to the best of our knowledge. We present a monotonic behavior of ϕ_B as a function of fiber length, which demonstrates, for the first time to our knowledge, the use of microstructured fibers as a dip sensor.

We assume that the power excited in the jth mode at excitation frequency ω^E can be expressed as [6]

$$P_j^E(z) = |a_j^E|^2 N_j^E \exp(-\gamma_j^E z), \tag{1}$$

$$\gamma_j^E = k(\epsilon_0/\mu_0)^{1/2}(1/N_j^E) \times \int_\infty \mathrm{Re}(n^E)\mathrm{Im}(n^E)|\mathbf{e}_j^E|^2 \mathrm{d}A, \tag{2}$$

where $\mathbf{e}_j^E(x,y)$, $\mathbf{h}_j^E(x,y)$, and β_j^E are the jth mode electric and magnetic field distributions and propagation constant, respectively; a_j^E is the amplitude; N_j^E is the power normalization factor of mode j [6]; and $\mathrm{Re}(n^E)$ and $\mathrm{Im}(n^E)$ are real and imaginary refractive indices. Here, we assume that γ_j represents all absorption mechanisms in the MOF, including absorption due to the Beer–Lambert law. Upon absorbing the excitation photons the fluorescent species in the holes behave as sources and emit fluorescent photons in all directions. This fluorescent emission can also be written [6] as the sum of forward, backward, and radiation modes with the consideration of power decay due to loss at the fluorescence frequency. Similar to the formalisms developed in [1], we have found that the fluorescent power contribution to the ith backward mode of the MOF at $z=0$ due to a small filled section $\Delta z = z_2 - z_1$ located at z' [see Fig. 1(a)] as

$$\mathrm{d}P_{-i}^F(0,z') = \frac{\pi \exp(-\gamma_i^F z')}{4\omega_F \mu_0 n_H^F k N_i^F} \int_A \int_{z_1}^{z_2} |\mathbf{e}_{-i}^F|^2 P_D \mathrm{d}A \mathrm{d}z''. \tag{3}$$

Here, $P_D(\mathbf{r})$ is the radiation power density of the fluorescent emission of the filling material [1,7], subscript $-i$ refers to the ith backward mode, and subscript H generally refers to the filled-hole region. By using Eq. (1)—assuming that the fluorescent power density is proportional to the density of excitation

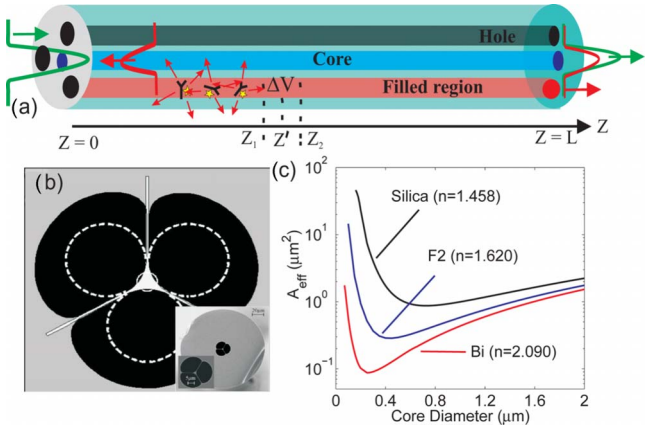

Fig. 1. (Color online) Schematic of a filled MOF showing (a) the parameters used in modeling and (b) the SEM image of the cross section of the MOF used for the modeling and experiment. (c) Effective area of the fundamental mode for the geometry shown in (b) when the holes are filled with Rhodamine B in an isopropanol solution. The wavelength is 590 nm, the refractive index of isopropanol is 1.3774, and the different substrate glasses are marked.

power loss due to the Beer–Lambert law in the filled region (proportionality constant ξ)—and evaluating the integrals in Eq. (3) with respect to z'', in the limit of $z_1 \to z_2$ and z' [see Fig. 1(a)], we find

$$\Phi_B = 2A \frac{1}{(\gamma_j^E + \gamma_i^F)} \{1 - \exp[-(\gamma_i^F + \gamma_j^E)L]\},$$

$$A = \frac{\xi \alpha_B \lambda^2 n_H^E \epsilon_0}{8\pi n_H^F \mu_0} \delta_j^E \frac{\int_H |\mathbf{e}_i^F|^2 \mathrm{Re}[(\mathbf{e}_j^E \times \mathbf{h}_j^{E*}) \cdot \hat{z}] \mathrm{d}A}{4 N_i^F N_j^E},$$

$$\Phi_F = 2A \frac{\exp(-\gamma_i^F L)}{(\gamma_j^E - \gamma_i^F)} \{1 - \exp[(\gamma_i^F - \gamma_j^E)L]\}. \quad (4)$$

Here, α_B is the Beer–Lambert absorption coefficient, $|\mathbf{e}_{-i}^F|^2 = |\mathbf{e}_i^F|$ [6]; $P_j^E(0)$ is the input excitation field power; the relation for $\Phi_F = P_i^F(L)/P_j^E(0)$ [1] is given for comparison with the $\Phi_B = P_{-i}^F(0)/P_j^E(0)$; and the factor 2 in Φ_F and Φ_B is due to the contribution from the two polarizations.

Next, we apply the developed model to an MOF, as shown in Fig. 1(b), with the following parameters: excitation wavelength $\lambda_E = 532$ nm, fluorescence wavelength $\lambda_F = 590$ nm, filling material: Rhodamine B dissolved in isopropanol, and three different glass materials [silica, lead silicate (F2), and bismuth]. We have used Rhodamine B simply to compare the results for forward and backward propagating modes. Simulation results of Φ_F and Φ_B as a function of fiber length, as shown in Fig. 2(a), indicate that while Φ_F maximizes at an optimum length, Φ_B increases rapidly for short lengths and then approaches an asymptotic value. The reason for the difference is clear: the fluorescent emission coupled to the backward mode can be detected instantaneously once the incident beam enters the filled region at $z = 0$ [(see Fig. 1(a)], while the emission coupled to the forward

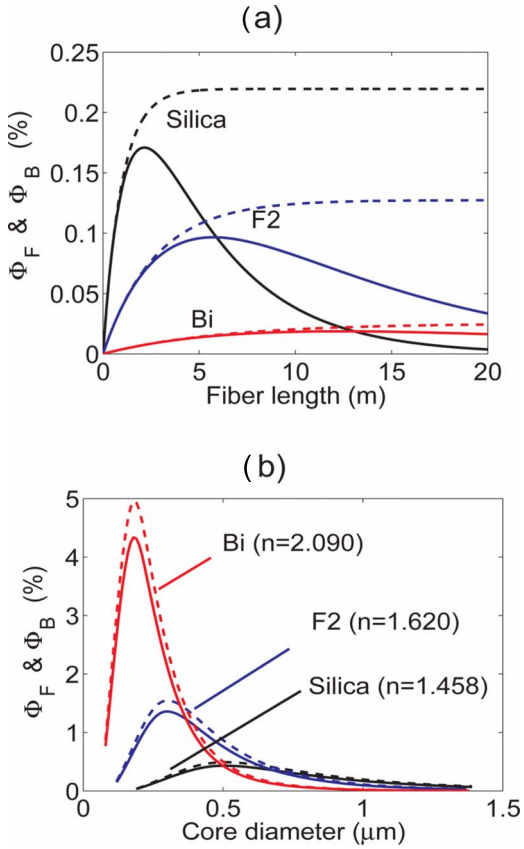

Fig. 2. (Color online) Numerical results of the fluorescence capture fraction for forward (Φ_F, solid curves) and backward (Φ_B, dashed curves) directions as a function of (a) fiber length and (b) core diameter for different substrate glasses. Other parameters are core diameter 1.0 μm in (b) and concentration 0.5 μM in (a) and (b). Φ_F and Φ_B in (b) correspond to the optimum fiber length defined at the maximum of Φ_F in (a).

mode needs to travel through the filled region, having a decay of $\exp(-\gamma^F L)$, to be detected at $z = L$. This is also evident from Eqs. (4); in the limit of $L \to \infty$ the Φ_F approaches zero but Φ_B approaches an asymptotic value. This demonstrates for the first time, to the best of our knowledge, that Φ_B can be advantageously employed for fluorescence sensing because of its higher efficiency and lower loss in comparison with Φ_F. Φ_B has other advantages over Φ_F including the possibility of using a dip-sensing configuration [see Fig. 3(a)], real time measurement, a higher signal to pump ratio, no optimal length (the longer the fiber length the higher the Φ_B), and ease of use in terms of keeping the launching end of the setup intact and using the exit end for filling.

In our previous publication we identified an interesting regime of small core diameters ($d < 0.8$ μm), for which the Φ_F can be significantly enhanced by employing high index (soft) glasses. The study of ϕ_B shows similar behavior as is evident from Fig. 2(b). For example, the maximum Φ_B for bismuth oxide fibers at $d \approx 0.18$ μm, is 4.96%, ten times larger than the maximum Φ_B value for silica fibers (0.50%) at $d \approx 0.52$ μm. Also, at the core size of $d \approx 0.2$ μm the maximum Φ_B value for bismuth fibers is 4.82%, 69

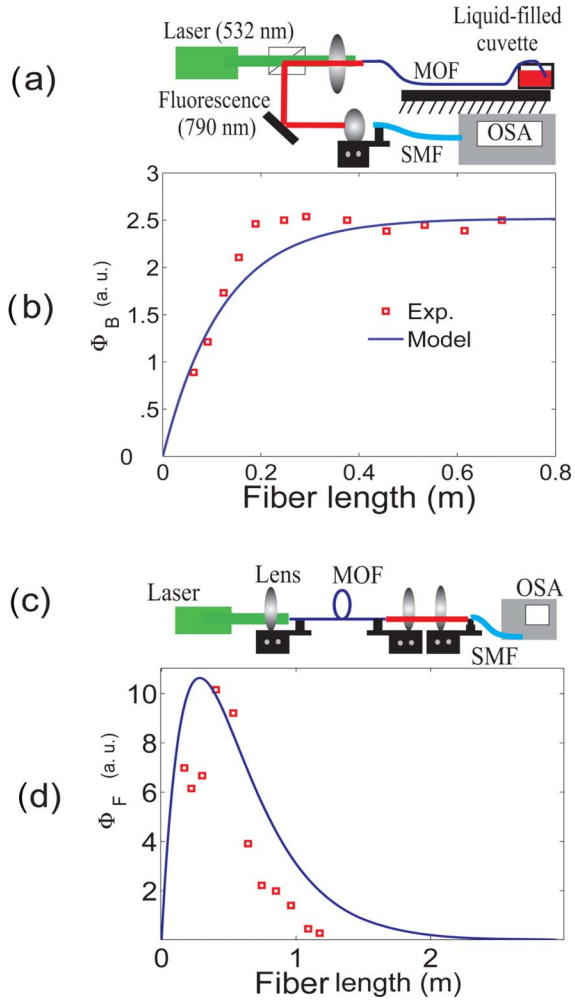

Fig. 3. (Color online) (a), (c) Experimental setups and results for measuring the fluorescence captured fraction into the (b) backward and (d) forward mode of an MOF with LLF1 substrate glass and a core diameter of 2 μm. The holes of the MOF are filled with a solution of 1 μM quantum dot. Simulation results are shown by solid curves (b) and (d).

times larger than that of silica fibers (0.07%). Similar to Φ_F [1], a thorough examination of Φ_B in Eq. (4) reveals that the sensitivity depends on both the power fraction in the holes and the intensity distribution of the modes. Therefore, fiber geometries resulting in high intensity regions may lead to high Φ_B even if they have a relatively smaller power fraction in the hole regions.

Figures 3(a)–3(d) show the experimental setup and results for measuring the fluorescence emission capturing into the backward [Figs. 3(a) and 3(b)] and forward [Figs. 3(c) and 3(d)] propagating modes as a function of fiber length. To the best of our knowledge, this is the first experimental investigation of length dependence of fluorescence capturing into the forward and backward modes of an MOF. We used MOFs similar to the one in Fig. 1(b) with substrate glasses of LLF1 ($n=1.55$) and core diameters and losses of approximately $d=2$ μm and 30 dB/m (filled fiber) at an excitation wavelength of 532 nm, respectively. The holes of the MOF were filled with an aqueous solution with 1 μM of CdTe–ZnS quantum-dot labeled goat F(ab')2 antimouse IgG conjugate from Invitrogen [8]. Experimental results qualitatively confirm the behavior of Φ_B and Φ_F as a function of length as predicted by the model. The model's results for Φ_B and Φ_F have been scaled individually to fit the experimental data. Better quantitative agreement may be achieved by having more accurate measurements of the fiber loss, quantum dot concentrations, fiber core diameter, and the loss due to mode mismatching between filled and unfilled sections of the MOF and by improving the stability and repeatability of light coupling into and out of the fiber especially for the forward approach.

A previous model of both in-fiber excitation and fluorescence recapturing of filled solid-core MOFs by their forward propagating modes [1] is generalized to include the capturing of fluorescence emission into the backward modes. Also, the capturing of fluorescence emission power into both forward and backward propagating modes of an MOF as a function of fiber length has been experimentally demonstrated and qualitatively confirmed with those of the numerical model. The numerical results presented here also demonstrate for the first time to our knowledge that the fluorescence emission coupled into the backward modes has a higher efficiency than those of the forward modes. This, however, can be confirmed experimentally by using optimized outcoupling setups or advanced coupling techniques such as tapers or high numerical aperture buffer fibers. Considering the advantages of Φ_B over Φ_F such as higher efficiency, higher signal to pump ratio, possibility of using a dip-sensing configuration [see Fig. 3(a)], ease of use in terms of experimental setup, and the previous results of our group, reporting the detection of quantum dots with a concentration as low as 1 nM using the forward approach [5], we expect to improve our detection power to picomolar concentration using our new backward approach with optimized coupling setups.

We acknowledge the Defence Science and Technology Organization (DSTO), Australia, for supporting research in the Centre of Expertise in Photonics. This research was supported under the Australian Research Council's Discovery Projects funding scheme (project DP0665486).

References

1. S. Afshar V., S. C. W. Smith, and T. M. Monro, Opt. Express **15**, 17891 (2007).
2. M. Nagel, A. Marchewka, and H. Kurz, Opt. Express **14**, 9944 (2006).
3. G. S. Wiederhecker, C. M. B. Cordeiro, F. Couny, F. Benabid, S. A. Maier, J. C. Knight, C. H. B. Cruz, and H. L. Fragnito, Nat. Photonics **1**, 115 (2007).
4. R. E. Bailey, A. M. Smith, and S. Nie, Physica E (Amsterdam) **25**, 1 (2004).
5. Y. Ruan, E. P. Schartner, H. Ebendorff-Heidepriem, P. Hoffman, and T. M. Monro, Opt. Express **15**, 17819 (2007).
6. A. W. Snyder and J. D. Love, *Optical Waveguide Theory* (Chapman and Hall, 1995).
7. D. Marcuse, J. Lightwave Technol. **6**, 1273 (1988).
8. http://probes.invitrogen.com/products/qdot/.